

Eta-Virginids: another asteroidal meteoroid stream

Jiří Borovička^{a,*}, Pavel Spurný^a, Pavel Koten^a, Gabriel Borderes Motta^a, Lenka Kotková^a, Rostislav Štork^a, Dušan Tomko^b and Thomas Weiland^c

^aDepartment of Interplanetary Matter, Astronomical Institute of the Czech Academy of Sciences, Fričova 298, 25165 Ondřejov, Czech Republic

^bAstronomical Institute of the Slovak Academy of Sciences, 05960 Tatranská Lomnica, Slovak Republic

^cÖsterreichischer Astronomischer Verein, Treumanngasse 5, 1130 Wien, Austria

ARTICLE INFO

Keywords:
Asteroids
Meteoroids
Meteor showers

ABSTRACT

Eta-Virginids is a less-known meteor shower active in March. We investigated the meteoroids of this shower using fireball data from the European Fireball Network supplemented by video data of faint meteors. We first derived the criteria for assigning meteors to this shower. A fragmentation model was then applied to selected shower fireballs with good deceleration data and light curves. Meteoroid fragmentation strengths and bulk densities were derived and compared with three other showers. We have confirmed the four year periodicity in the activity of η -Virginids and their presence in the 3:1 mean motion resonance with Jupiter. The orbital period of four years was directly measured for the fireballs. Fainter meteors showed somewhat longer periods but the shower is poor in faint meteors. No member fainter than magnitude +1 was observed instrumentally. The physical properties of meteoroids are different from cometary streams and are similar to the Geminids. The limiting fragmentation strength of 0.5 MPa and typical bulk density of cm-sized meteoroids of 1500 kg m^{-3} suggest that the parent body is a carbonaceous asteroid. Besides Geminids, η -Virginids is another stream of asteroidal origin. Some small meteoroids have densities around 2500 kg m^{-3} . Three asteroids of the sizes between 40 – 120 meters have been found to have similar orbits but their relation to η -Virginids remains uncertain.

1. Introduction

A meteor shower occurs when the Earth passes through a meteoroid stream. Meteoroid streams are formed by meteoroids on similar orbits having a common origin. In most cases, when the parent body of a meteoroid stream is known, it is a comet (Ye and Jenniskens, 2024). The notable exception are Geminids whose parent body is asteroid (3200) Phaethon. Another meteoroid stream connected with an asteroid, the Daytime Sextantids connected with (155140) 2005 UD, is part of the same Phaethon-Geminid complex. The Quadrantids are related to asteroid (196256) 2003 EH₁ but both are part of the Machholz Interplanetary Complex which also contains comet 96P/Machholz. Other 21 meteor showers listed by Ye and Jenniskens (2024) are linked directly to comets.

The mechanisms how comets produce meteoroid streams are well understood. The meteoroids are ejected by gas drag during the sublimation of ices, that means during the normal cometary activity. Large amount of meteoroids can be also released during sub-catastrophic or catastrophic break-ups comets which comets sometimes undergo from various reasons (Knight et al., 2024). On the contrary, the formation mechanism of meteoroids within the Phaethon-Geminid complex is still debated. One possibility is that Phaethon is an extinct comet and the meteoroids were produced by normal cometary activity (e.g. Ryabova, 2016). Other possibilities include thermal decomposition and fracture (Jewitt and Li, 2010), rotational instability (Jo and Ishiguro, 2024) or an unspecified catastrophic event near perihelion (Cukier and Szalay, 2023). Phaethon has a quite low perihelion distance (0.13 AU) and a faint tail was observed when the asteroid is close to the Sun (Jewitt et al., 2013). The tail, however, does not consist of solid material. It is formed by sodium thermally desorbed from the asteroid (Zhang et al., 2023).

The nature of the parent body can be judged from the physical properties of meteoroids. It has been discovered long time ago that cm-sized meteoroids entering Earth's atmosphere differ enormously in their penetration ability (Ceplecha and McCrosky, 1976). Meteoroids coming from the asteroid belt penetrate deep and can drop meteorites under favorable conditions. Meteoroids of cometary origin, for example members of cometary meteor showers, disintegrate

*Corresponding author

 jiri.borovicka@asu.cas.cz (J. Borovička)
ORCID(s): 0000-0002-5569-8982 (J. Borovička)

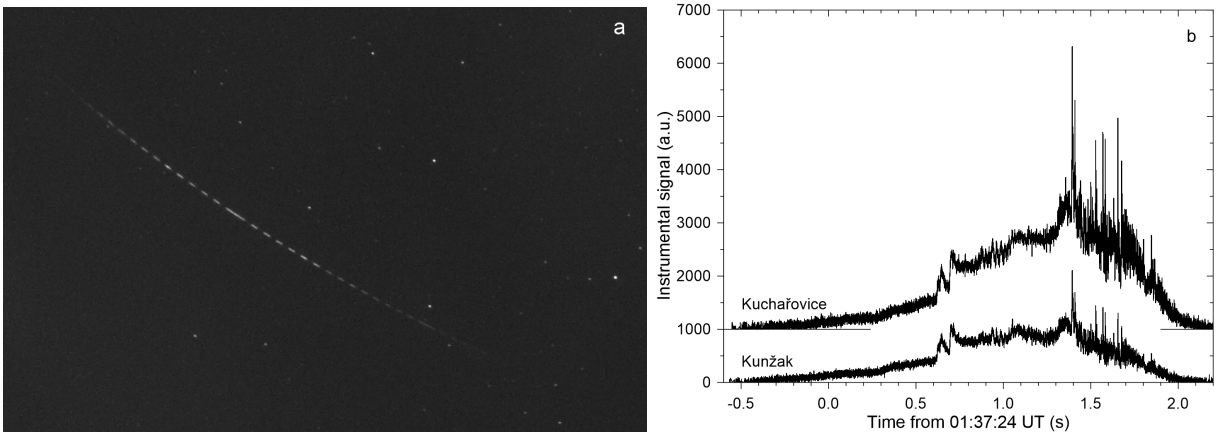


Figure 1: Eta Virginid fireball EN230321_013723 as photographed in constellation of Hercules by DAFO at station Kunžak (panel a) and by radiometers at Kunžak and Kuchařovice (b). The sky was partly hazy that night. The breaks in the fireball image are due to the LCD shutter. One break is intentionally avoided at the beginning of each second. The radiometric light curve from Kuchařovice has been offset by 1000 units for clarity.

high in the atmosphere. Ceplecha and McCrosky (1976) classified meteoroids into four types, I, II, IIIA, and IIIB, according to the fireball end heights. More recently, Borovička et al. (2022a) introduced classes Pf-I to Pf-V according to the maximum dynamic pressure reached during the atmospheric flight. According to both classifications, most large Geminids belong to the strongest class I and Pf-I, respectively. It was noted previously that Geminids contain the strongest meteoroids among all meteoroid streams (Spurný, 1993; Trigo-Rodríguez and Llorca, 2006; Babadzhanov and Kokhirova, 2009). That fact suggested an asteroidal nature of Phaethon. However, a possibility remains that meteoroids acquired their strength by a sintering process in the vicinity of the Sun (Halliday, 1988).

Besides simple indicators such as Pf, meteoroid physical properties can be studied by more detailed methods. Recently, Henych et al. (2024) modeled Geminids using the semi-empirical fragmentation model of Borovička et al. (2020) using genetic algorithms. They found that Geminids are stronger than the CM2 carbonaceous meteorite Winchcombe but weaker than asteroidal meteoroids (presumably ordinary chondrites) and concluded that Geminids are composed of compact carbonaceous material. Earlier, the same model was used by Borovička and Spurný (2020) for Taurids that originate from comet 2P/Encke and are much weaker.

In this paper, we study the less-known meteoroid stream η -Virginids. Our previous work (Brček et al., 2021; Borovička et al., 2022a) indicated that η -Virginid meteoroids are comparable in strengths with Geminids. Also Shiba (2018) noted that bright η -Virginids have lower ending heights in comparison with sporadic meteors of similar velocities. The orbits of η -Virginids do not have such a low perihelion distance as Geminids and the meteoroids are much less affected by solar radiation. Their parent body is not known. The aim of this work is to study the material properties of η -Virginids in detail using the semi-empirical fragmentation model and to reveal the nature of their parent body. Since the radiant and low-inclination orbit of this shower is not markedly distinct from many sporadic meteors of asteroidal origin, we first need to recognize which meteors belong to η -Virginids without any doubt.

2. Observational data

We primarily use fireball data obtained within the European Fireball Network (hereafter EN) (Spurný et al., 2017; Borovička et al., 2022b) in the years 2017–2025. The main instrument is the Digital Autonomous Fireball Observatory (DAFO). DAFO takes all-sky digital photographs every clear or partly clear night. The exposure length is 35 s and the exposure is interrupted 16 times per second by an electronic Liquid Crystal Display (LCD) shutter to enable fireball velocity measurement (Fig. 1a). The limiting magnitude of DAFO under good conditions (dark clear night, meteor high in the sky) is about -2 . DAFOs are currently placed at 20 stations in the Czech Republic (15), Slovakia (4) and Austria (1). Combining DAFO images from at least two stations enables us to compute the fireball trajectory, entry velocity, deceleration along the trajectory due to atmospheric drag, light curve with time resolution of $1/16$ s, and heliocentric orbit. DAFO is further equipped with a radiometer measuring the light intensity from the whole sky with

time resolution of 1/5000 s. Radiometers are sensitive from magnitudes about -3 though the full time resolution can be used only for fireballs of magnitude -6 and brighter. The radiometric curves in Fig. 1b demonstrate that fireball light curves can be more complex than it seems from the photographs.

To increase the precision of the data, DAFO observations were supplemented by data from other observational systems within the EN. Spectral version of DAFO, called SDAFO, has been installed at half of the stations plus one station in Germany. It has a lens with longer focal length but no LCD shutter. Besides taking spectra of bright fireballs, SDAFO images can be used to improve the trajectory solutions, but not velocities. No η -Virginid spectrum was captured.

All stations have been also equipped with at least one Internet Protocol (IP) video camera taking 20 or 25 frames per second. IP cameras cover only part of the sky but are more sensitive than DAFOs and can therefore record fireballs for a longer time. They are very useful for improving the velocity solutions and thus also the heliocentric orbits.

In this work, we also intended to study some faint η -Virginid meteors. For that purpose, a double-station observing campaign using sensitive image intensified video cameras was organized during three clear nights in March 2025 (March 18–20). Second generation image intensifiers Mullard XX1332 equipped with 1.4/50 mm lenses providing circular field of about 50° were used in Ondřejov and Kunžak. The videos with resolution 1280×960 pixels and 30 frames per second were taken with digital DMK23G445 GigE monochromatic cameras and recorded with no compression on personal computers. The limiting magnitude for meteors was about $+5$.

The methods of data reduction are described in most detail in Borovička et al. (2022b). More information about the video system can be found in Koten et al. (2023).

3. Identification of η -Virginids

3.1. History

Eta Virginids are listed as an established meteor shower with number 11 and code EVI in the Meteor Shower Database of the International Astronomical Union (IAU MDC, Hajduková et al., 2023). Apart from earlier visual observations, the shower named Virginids, with an orbital period of 4 years, was mentioned by Whipple (1954) in a study of meteor orbits obtained by small photographic cameras. Jacchia and Whipple (1961) marked three meteors as possible Virginids among 413 meteors photographed by more sensitive Super-Schmidt cameras, while McCrosky and Posen (1961) considered five meteors from 2,539 meteors photographed by the same cameras to be Virginids. The radiants and orbits of these eight meteors varied widely. Lindblad (1971) performed a computer search for meteor showers in the catalog of McCrosky and Posen (1961) and designated four meteors as Northern Virginids and three meteors as Southern Virginids. From these seven meteors, only three were labeled as Virginids by McCrosky and Posen (1961).

In his first book, Jenniskens (2006) named the shower η -Virginids. He included showers claimed by various authors to be active in March in Virgo under that name. Most of those showers had a low number of observed meteors. Some were based on radar techniques. He also listed Southern March Virginids (SVI) and Northern March Virginids (NVI) as separate showers with even longer period of activity and corresponding to the antihelion source. The first good characterization of η -Virginids come from video observation of 56 shower members during a week in March 2013 (Jenniskens et al., 2016). The shower had a narrow distribution of radiants in ecliptic latitude but extended in longitude. The mean orbital elements had a semimajor axis $a = 2.47$ AU corresponding to period 3.9 years, perihelion distance $q = 0.46$ AU, and inclination $i = 5.4^\circ$.

A major progress was done by Shiba (2018) who analyzed Japanese video data obtained between 2007 – 2018. He found a four year cycle in meteor activity with the highest η -Virginid activity being observed in the years 2009, 2013, and 2017, somewhat lower activity in the following years 2010, 2014, and 2018 and no activity in the remaining years. He proposed existence of a meteoroid swarm in 3:1 mean motion resonance with Jupiter. The corresponding orbital period is 3.95 years. The orbital elements of individual meteors, however, exhibited significant scatter. The mean orbital period was only 3.58 yr, which was attributed to calculation errors. Jenniskens (2023) confirmed the four-year periodicity in activity though he detected the shower every year.

3.2. EN data

Eta Virginids obviously overlap with the antihelion source of sporadic meteors. We used EN data to develop strict criteria to assign meteors to the shower. Figure 2a shows geocentric radiants and velocities of all fireballs observed between March 1–31 of all studied years and having radiants in the Virgo region. The only concentration of radiants is

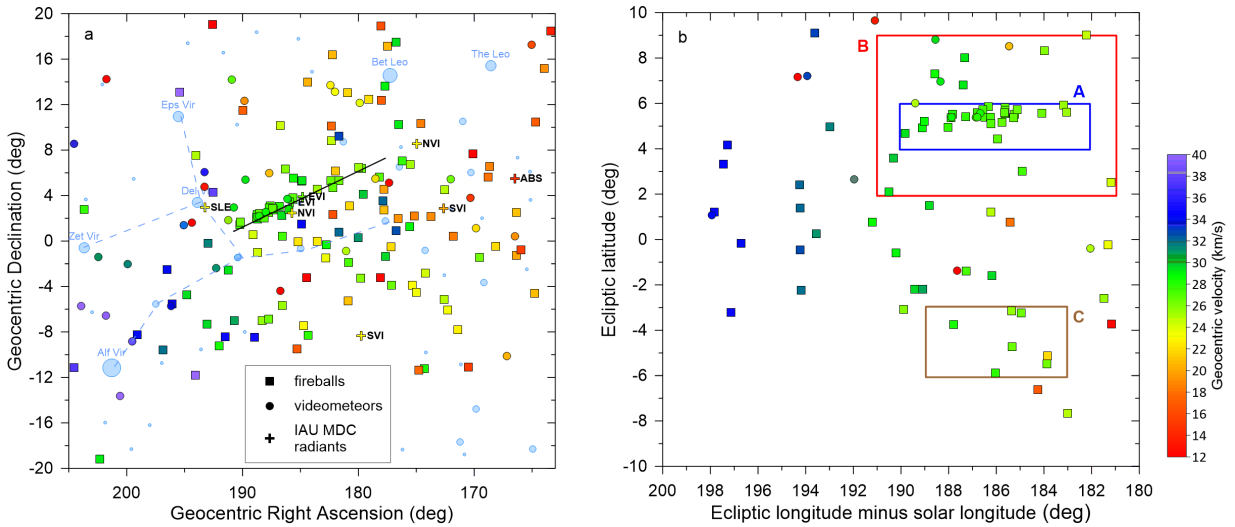


Figure 2: Positions of geocentric radiants located in the Virgo region in equatorial coordinates (panel a) and in Sun-centered ecliptical coordinates (b). The radiants of all fireballs observed by the EN during the month of March in 2017–2025 are plotted as color squares. The radiants of video meteors observed during three nights in March 2025 are plotted as color circles. The radiants of meteor showers active in March according to the IAU MDC are plotted as crosses in panel a. (NVI = Northern March Virginids, SVI = Southern March Virginids, EVI = η -Virginids, SLE = σ -Leonids, ABS = April β -Sextantids) Some showers have multiple solutions in the database and thus more possible radiants. Geocentric velocities are color coded. Stars are plotted as light blue circles. The black line marks the concentration of radiants. Three regions of interest are marked by rectangles in panel b: radiant concentration (A), wider area around the concentration (B) and possible southern branch (C).

along the marked line and overlaps with the cataloged radiant of η -Virginids according to two sources. One cataloged radiant of Northern March Virginids is also close but the velocity is different. We therefore definitely detected η -Virginids in our sample. To study their physical properties, we must distinguish them from sporadic fireballs with similar radiants.

The radiants are plotted in Fig. 2b in Sun-centered ecliptical coordinates, namely ecliptical longitude minus solar longitude ($\lambda - \lambda_{\odot}$) and ecliptical latitude (β). The region of radiant concentration (marked A) is narrow in β and prolonged in $\lambda - \lambda_{\odot}$, as noted already by Jenniskens et al. (2016). We will investigate further if meteors from a wider region (marked B) may also belong to η -Virginids. In addition, since Shiba (2018) and Brček et al. (2021) mentioned a possible southern branch, we also investigated a region on the opposite side of the ecliptic (marked C). Some meteors in these additional regions have obviously deviating velocities but several have velocities roughly consistent with η -Virginids.

We further investigated semimajor axes or, equivalently, orbital periods. Orbital periods of meteors with radiants in regions A, B, C are plotted in Fig. 3 versus solar longitude, i.e. the time of meteor appearance. We can see that all fireballs in region A appearing between solar longitudes $350^\circ - 3^\circ$ (nearly March 10 – 23) had orbital periods very close to four years. One fireball appearing in this region earlier and one appearing later had different periods and we therefore do not consider them to belong to η -Virginids. Fireballs of regions B and C show much larger scatter in both solar longitude and period and we also do not consider them to belong to η -Virginids, though three fireballs of region B and one of region C fall, probably by chance, within the right limits of solar longitude and period.

In summary, our working hypothesis is that only fireballs appearing at λ_{\odot} between 350° and 3° , having radiants with β between 4° and 6° and $\lambda - \lambda_{\odot}$ between 182° and 191° , and orbital periods between 3.8 – 4.2 years are with high probability true η -Virginids. Note that from eight marked as Virginids in the Super-Schmidt data by Jacchia and Whipple (1961) and McCrosky and Posen (1961), only two (meteors no. 6798 and 6949) can be considered to be η -Virginids according to their radiants. A similar conclusion was reached by Koseki (2019). In our previous work (Brček et al., 2021), EN060319_204604 was incorrectly considered to be an η -Virginid.

Eta-Virginid meteoroid stream

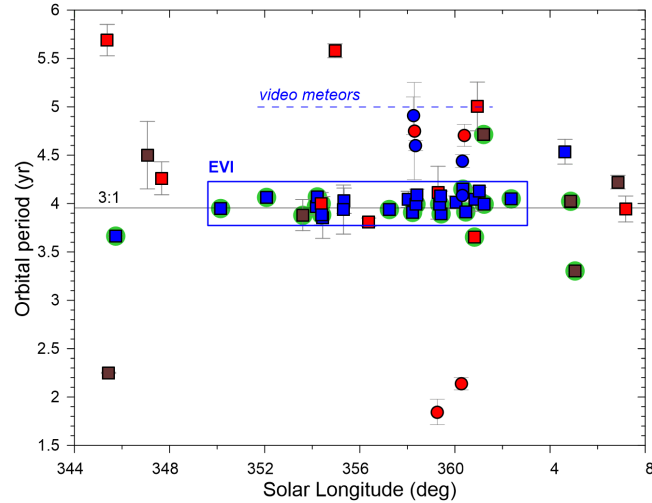


Figure 3: Orbital periods versus solar longitude of meteors with radiants in regions A (blue), B (red), and C (brown). EN fireballs are plotted as squares, video meteors as circles. Video data, generally, have somewhat lower precision. Error bars of orbital periods are indicated (one sigma). The horizontal line corresponds to the 3:1 resonance with Jupiter. The blue rectangle is the region of η -Virginid fireballs. The dashed blue line indicates possible extension of orbital periods of η -Virginid video meteors. The fireballs which were subject to fragmentation modeling (see Sect. 6) are highlighted by green circle.

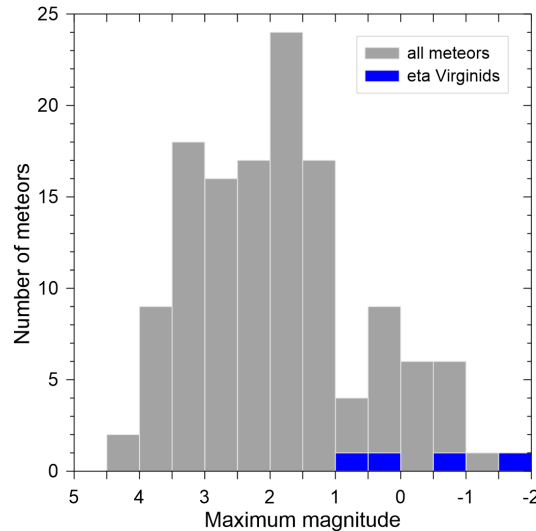


Figure 4: Magnitude distribution of all 130 meteors observed by video cameras during three nights in March 2025 and of four η -Virginids among them.

3.3. Video data

In total, 130 double-station meteors were observed by the video experiment in three clear nights in March 2021 (at solar longitudes $358^\circ - 0.5^\circ$). They are included as circles in Figs. 2 and 3. Only four meteors had radiants in region A, four in B, and none in C. Only one meteor had the period close to 4 years. The other three meteors from region A had periods between 4.4 – 4.9 years. Nevertheless, we consider them as probable η -Virginids. It is possible that small meteoroids have larger semimajor axes from some reason, for example the influence of radiation pressure (Burns et al., 1979) or larger ejection velocities during stream formation. All four η -Virginids were brighter than magnitude +1 while large majority of other meteors were fainter than +1 (Fig. 4). It therefore seems that η -Virginids contain very

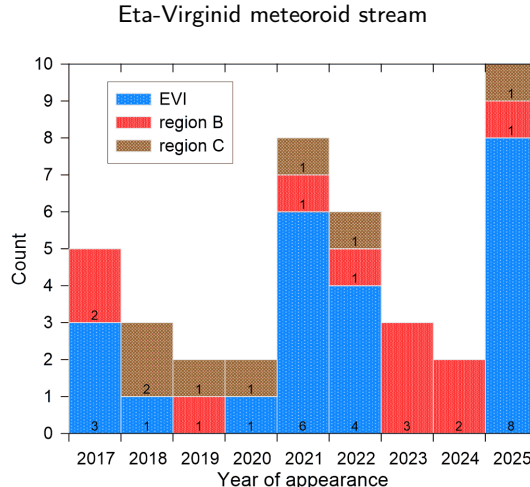


Figure 5: Number of EN fireballs observed in each year. The confirmed η -Virginids are in blue. Fireballs with radiants in region B and those with radiants in region A but orbital periods incompatible with η -Virginids are in red. Fireballs with radiants in region C are in brown.

few faint meteors. The two Super-Schmidt η -Virginids (6798 and 6949) were both brighter than zero magnitude. On the other hand, during the visual observations by one of us (TW) on four clear nights in 2021 (16/17 to 20/21 March), 10 of the 18 observed η -Virginids were fainter than +1 mag (down to +5). Nevertheless, the magnitude distribution was quite flat.

4. Periodic activity

As we have now identified the true η -Virginids, we can look in which years they were active. The distribution was not random (Fig. 5). A larger number of fireballs was observed in 2017, 2021, 2022, and 2025. One η -Virginid was observed in 2018 and 2020. We can therefore confirm the observation of Shiba (2018) that η -Virginids are always active in two consecutive years and no activity occurs in the next two years. This four-year cycle is in full agreement with the 4 year orbital period we have found. The only fireball which occurred in 2020 when no activity was expected was EN190320_201746. As we will see in Sect. 6, that meteoroid had different physical properties than the rest of η -Virginids. It is therefore possible that it was a random interloper and not a shower member.

Fireballs with radiants in regions B and C (see Fig. 2b) are also shown in Fig. 5. They occurred randomly and are not correlated with η -Virginids. That fact confirms that they did not belong to the shower.

5. Radiants and orbits

We present in this section the mean radiants and orbits of η -Virginids based primarily on the photographic EN data. The motion of the mean geocentric radiant with solar longitude λ_{\odot} can be expressed as

$$\alpha_g = 186.1^\circ + 0.97 \cdot (\lambda_{\odot} - 358^\circ) \quad (1)$$

$$\delta_g = +3.3^\circ - 0.38 \cdot (\lambda_{\odot} - 358^\circ), \quad (2)$$

where α_g is the right ascension and δ_g is the declination of the geocentric radiant. The shower was observed active between solar longitudes 350° and 3° (March 10 – 23). For solar longitudes between zero and several degrees, 360° must be added to use the above equations. The radiant motion is depicted graphically in Fig. 6.

The radiant motion follows the motion of the Sun along ecliptic. As shown in Fig. 2b, the spread in ecliptic latitude is low, about 1.5° . The spread in ecliptic longitude related to the solar longitude is 7° . The spread is closely related to the spread of geocentric velocities and perihelion distances, as shown in Fig. 7. The fireballs with radiants more to the east from the antisolar point have larger velocities and lower perihelion distances. The linear dependencies are very well defined for EN fireballs. Some of video meteors lie somewhat off. The ranges of geocentric velocities ($25.5 - 29.5 \text{ km s}^{-1}$) and perihelion distances ($0.38 - 0.51 \text{ AU}$) are relatively large which contrasts with the narrow range of semimajor axes, and thus orbital periods, of the fireballs (Fig. 3). Similar linear dependencies exist also for the

Eta-Virginid meteoroid stream

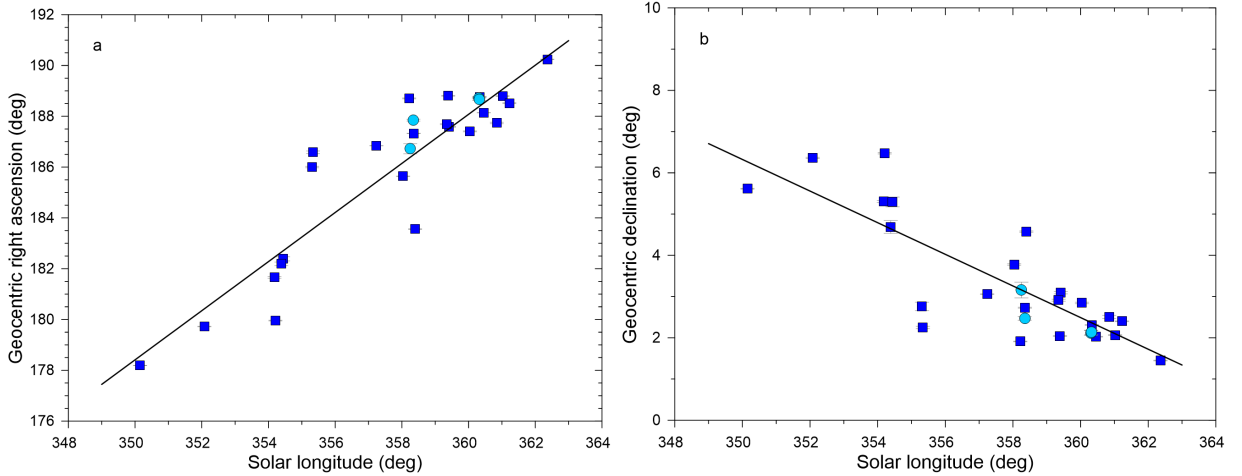


Figure 6: Right ascension (a) and declination (b) of geocentric radiant as a function of solar longitude. EN fireballs are shown as squares, video meteors as circles.

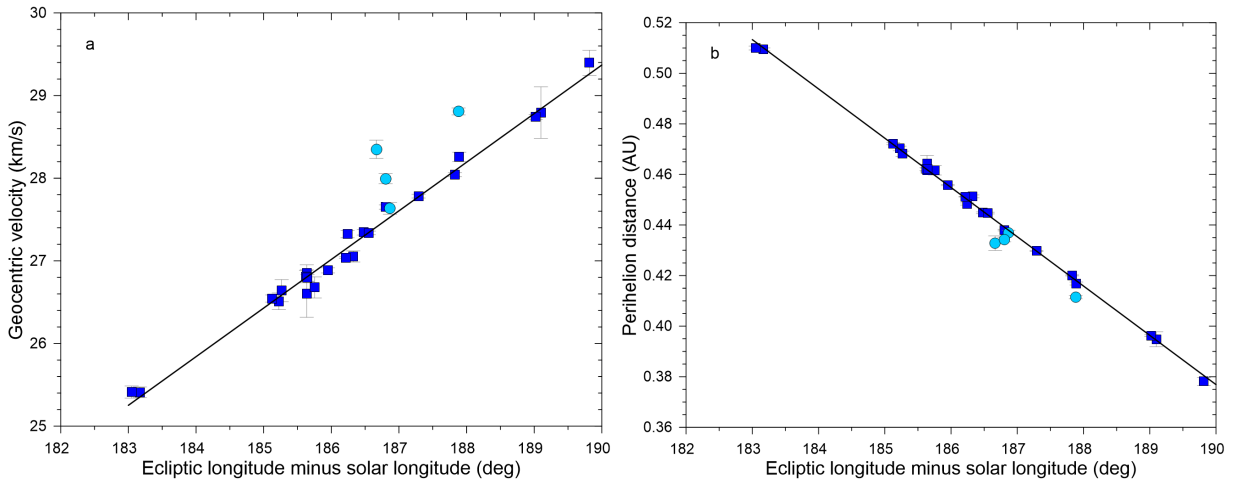


Figure 7: Geocentric velocity (a) and perihelion distance (b) as a function of Sun-centered ecliptical longitude of the radiant. EN fireballs are shown as squares, video meteors as circles.

Table 1
Mean orbital elements of 23 η -Virginid fireballs (J2000.0)

Semimajor axis AU	Eccentricity	Perihelion distance AU	Aphelion distance AU	Inclination degrees	Argument of perihelion degrees	Longitude of ascending node degrees
2.52	0.82	0.45	4.6	5.5	283	358

eccentricity and the argument of perihelion. Inclinations are in a narrow range, $5 - 6^\circ$ for most fireballs and meteors; only one fireball with $i = 4.38^\circ$ deviates markedly.

The orbits are shown graphically in Fig. 8. Table 1 contains the mean orbital elements based on the fireball data. The mean elements are similar to those obtained by Shiba (2022). We must, nevertheless, keep in mind that most elements, except semimajor axis and inclination, exhibit significant natural spread, which is not due to observational errors. The range of eccentricities is 0.80 – 0.85, and of arguments of perihelion $276 - 290^\circ$. Fainter meteors observed by video cameras show also a spread in semimajor axes.

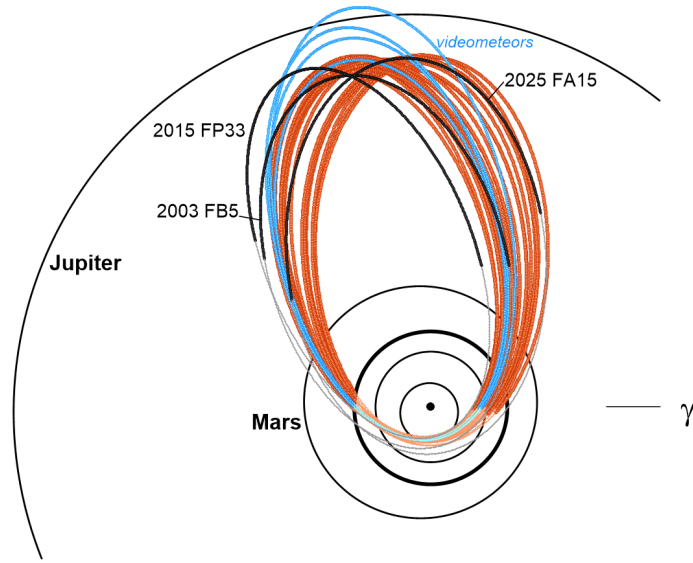


Figure 8: Orbits of all observed η -Virginids in the projection to the plane of ecliptic. EN fireballs are in red and video meteors in blue. The thin lines depict the parts of orbits below (to the south of) the ecliptic. The three black/gray curves show the orbits of three asteroids with orbits most similar to η -Virginids. The position of the Sun, the orbits of planets from Mercury to Jupiter, and the direction to the vernal equinox are also shown.

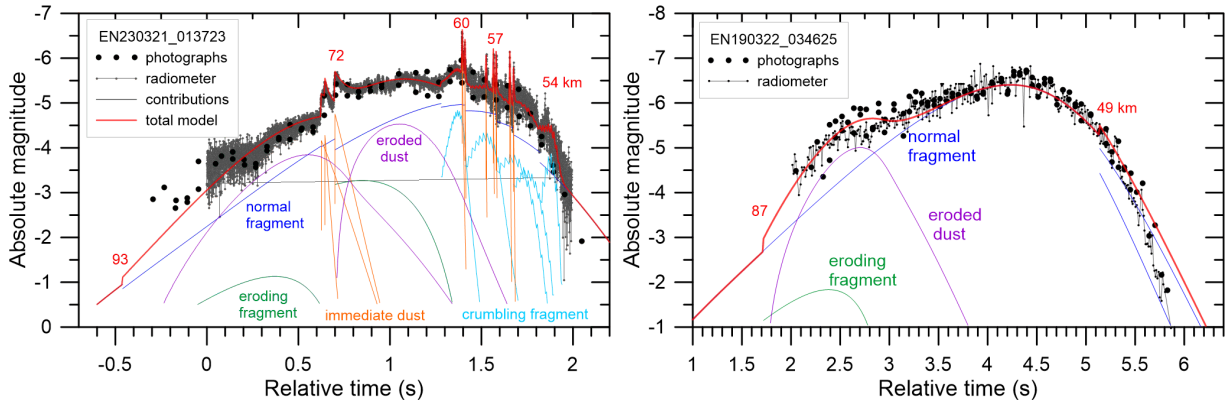


Figure 9: Observed and modeled light curves of η -Virginid fireballs EN230321_013723 and EN190322_034625. Individual contributors to the model are shown. The numbers are heights of selected fragmentation events in km. The zenith angle of EN230321_013723 was 52° ; in case of EN190322_034625 it was 67° .

6. Physical properties

6.1. Fragmentation modeling

The main goal of this paper is the evaluation of physical properties of η -Virginid meteoroids, namely fragmentation strengths and bulk densities. As in our previous work on Taurids (Borovička and Spurný, 2020), we used the semi-empirical fragmentation model. The model has been described in detail in Borovička et al. (2020). The fitting of the observed light curves and decelerations was done manually. The free parameters were the initial mass, velocity, and density of the meteoroid and the description of the fragmentation process during the atmospheric flight.

The outputs of each fragmentation event could be normal individual fragments, a group of fragments of identical masses, immediately released dust, an eroding fragment releasing dust gradually, or a crumbling fragment undergoing progressive fragmentation. The ablation coefficient of all fragments and dust particles was kept constant at $\sigma = 0.005 \text{ s}^2 \text{km}^{-2}$, the product of the drag and shape coefficient was assumed to be $\Gamma A = 0.8$, the density of the dust particles was 2000 kg m^{-3} , and the mass distribution index of the dust particles was $s = 2.0$. The erosion coefficient and the upper and lower mass limit of the dust, either eroded or immediately released, was to be adjusted. The crumbling fragment is a new feature of the model describing schematically fragments which are fragmenting in a cascade. It is assumed that each created fragment is fragmenting further after a fixed time interval into a fixed number of fragments. The number of fragments in the cascade therefore grows geometrically and the masses of all fragments are identical at any time instant. The free parameters are the time interval of fragmentation, the number of daughter fragments, and the mass limit at which the fragmentation stops. The used atmospheric density and luminous efficiency model is described in Borovička et al. (2020).

As an example, Fig. 9 shows the light curve of fireball EN230321_013723 which was imaged in Fig. 1. While the light curve looks smooth on the photograph, the radiometer revealed a number of short flares with the amplitude of about one magnitude. They could be well modeled by immediate dust releases. In overall, the fragmentation was quite complex and both eroding fragments and crumbling fragments were needed to explain the light curve. On the other hand, another fireball displayed in Fig. 9, EN190322_034625, had a really smooth light curve with only a hump at the beginning, explained by erosion. There was also a fragment splitting near the end at the height of 49 km which was not demonstrated on the light curve but was needed in the model to explain the increase of deceleration at the end.

In both fireballs, a fragmentation before the beginning of our instrumental records, at the heights around 90 km, was needed to explain the shape of the light curve at the beginning. The created eroding fragment contained 10 – 15% of the original mass. It may represent an incoherent surface layer of the meteoroid. Such effect was observed in a majority, but not all, η -Virginids.

Among 23 confirmed η -Virginid fireballs, 14 fireballs had good enough data for fragmentation modeling. In addition, we modeled for comparison seven fireballs which were excluded from the η -Virginid list on the basis of their radiants or orbital periods. Four of them have radiants in the southern region C. The modeled fireballs are highlighted in Fig. 3. To evaluate the strength of the meteoroids, we computed the dynamic pressures, p , at the time of fragmentation events. The pressure was computed as $p = \rho v^2$, where ρ is atmospheric density and v is fireball velocity. As in many similar studies, the role of the drag coefficient Γ was ignored, since its actual value is not known but it is of the order of unity.

6.2. Fragmentation strength

Figure 10 shows the mass of the largest remaining fragment during the penetration through the atmosphere as a function of increasing dynamic pressure for all modeled η -Virginids. Sudden drops of mass are due to fragmentation, gradual decrease is due to either erosion or ablation. The phases when the dynamic pressure decreased toward the end of the fireball are not shown. The curves belonging to the two fireballs in Fig. 9 are identified. The last fragmentation of EN190322_034625 occurred at the time when dynamic pressure reached the maximum.

We can see that small η -Virginids reach maximum dynamic pressure 0.1 – 0.2 MPa and large ones up to 0.5 MPa. The exception was the smallest meteoroid EN190320_201746 which was destroyed well below 0.01 MPa. At the same time, it was the only η -Virginid which occurred outside the usual activity years, namely in 2020. Though its radiant and orbital elements perfectly match with η -Virginid, it was probably a random interloper with different origin and physical properties. It will be therefore excluded from further discussion. The largest η -Virginid EN210325_042444 with a mass of 3.2 kg was observed during twilight, only 35 minutes before sunrise. It was a 200 km long fireball with a slope of 15° to the horizontal reaching an absolute magnitude –11 and lasting for 7.4 seconds. The observed end height was 45.5 km. The dynamic data from IP cameras are good but there is no radiometric light curve.

In Fig. 11a, dynamic pressures at the first fragmentation, at the time when the mass of the largest fragment dropped to 10% of the original mass, and the maximum dynamic pressure reached are plotted as a function of the original mass. The theoretical maximum dynamic pressure which could be reached by a strong non-fragmenting η -Virginid of the given mass is also indicated. It was computed for a meteoroid density 3500 kg m^{-3} , $\sigma = 0.005 \text{ s}^2 \text{km}^{-2}$, $\Gamma A = 0.8$, and the average trajectory slope (35°) and entry speed (29 km s^{–1}) in our sample.

As we can see in Fig. 11a, the first but generally minor fragmentation started in small (< 0.02 kg) meteoroids at pressures below 5 kPa. Some of the larger meteoroids avoided any low-pressure disruption. With one exception, the 90% mass loss occurred just before the maximum pressure was reached. As for the maximum pressure, medium sized

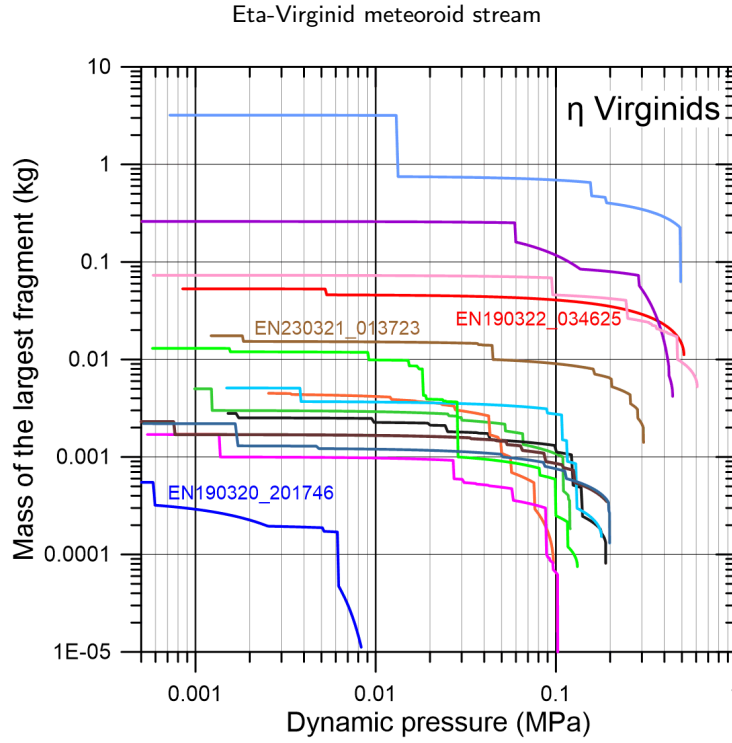


Figure 10: Mass of the largest remaining fragment as a function of increasing dynamic pressure for 14 modeled η -Virginids. Colors are used to distinguish individual meteoroids. The lines belonging to the two light curves shown in Fig. 9 and one very fragile meteoroid are labeled.

meteoroids with mass just below 0.1 kg proved to be the strongest, reaching the pressures of 0.5 MPa, which was close to the theoretical limit for their mass. They lost most mass by regular ablation with fragmentation playing a lower role. Larger meteoroids lost most mass in the form of eroding fragments and did not approach the theoretical maximum. It seems that 0.5 MPa is the material limit of η -Virginids.

The comparison of maximum pressures with those observed in three other meteor showers is presented in Fig. 11b. The Taurid data were taken from Borovička and Spurný (2020) and Geminid data from Henych et al. (2024). The identification of κ -Cygnid fireballs was recently done by Borovička et al. (2025). The details of their fragmentation modeling, done with the same methods as here, will be published elsewhere. They proved to be fragile bodies, obviously of cometary origin, reaching maximal pressures of only 8–80 kPa. Taurids are also of cometary origin but are stronger, typically 50–150 kPa. Some small Taurids of masses of about 10 grams are comparable with η -Virginids and Geminids of similar masses. Meteoroids of the Geminids and η -Virginids behave similarly. The strength increases with mass up to about 0.1 kg, where it reaches the maximum which does not increase further with mass. The maximum strength of Geminid meteoroids is higher than of η -Virginids, about 1.5 MPa, although there is no difference for small meteoroids. At few grams, η -Virginids may be even stronger than Geminids.

6.3. Bulk density

Another important quantity is the meteoroid bulk density. It is generally difficult to determine from meteor data. In our modeling, we were able to obtain reasonable values of meteoroid density combining both photometry and dynamics. A lower density means a larger cross section, which produces higher luminosity and larger deceleration. The luminosity can be used when the meteoroid is a single body – either before the first fragmentation or after the end of the initial erosion. Deceleration was not present at the beginning of the fireballs because of low atmospheric density. It started in the middle part. Assuming that the main fragment was a single body, deceleration could be used to determine the meteoroid density. In fact, the same deceleration could be alternatively produced by a body of higher density disrupted into several pieces. Deceleration therefore effectively provides a lower limit of density. Moreover, both luminosity and deceleration are affected by the values of parameters such as meteoroid shape and ablation coefficient. Nevertheless, obtaining a consistent solution for both photometry and deceleration provides some confidence that all parameters have

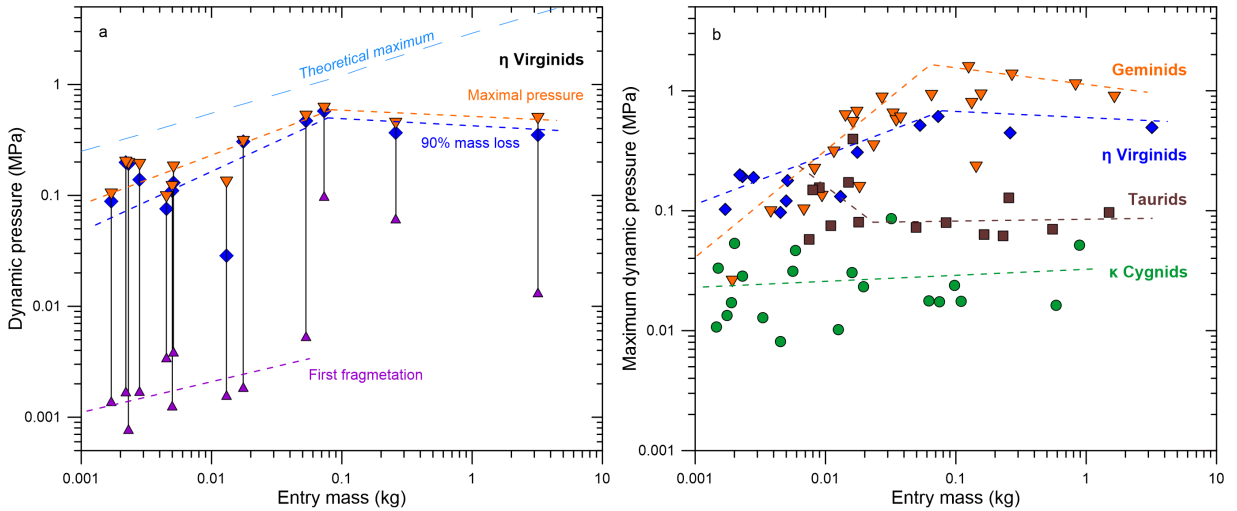


Figure 11: Selected dynamic pressures along the trajectories of all 13 modeled η -Virginid fireballs as a function of entry mass (panel a). The dashed lines are general trends, not exact fits to the data. The theoretical maximum was computed for hypothetical non-fragmenting and high-density η -Virginids. Panel b presents a comparison of the observed maximum pressure with three other representative showers, from strong Geminids to fragile κ -Cygnids.

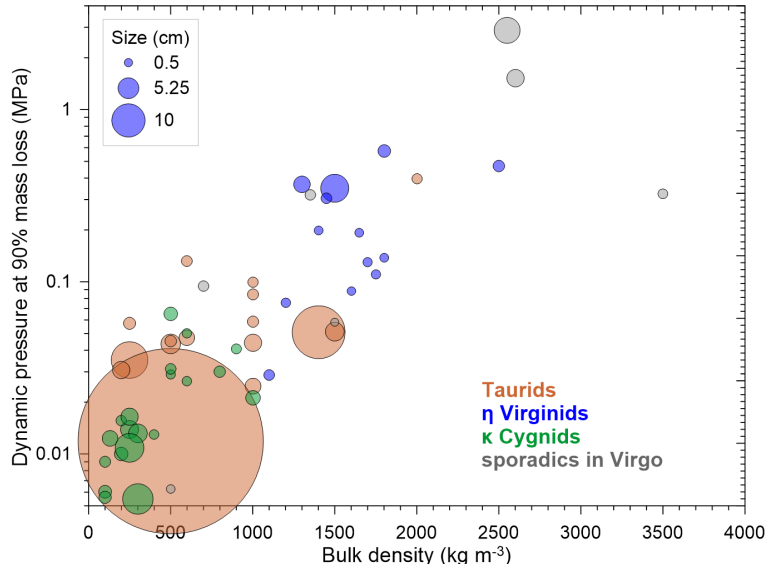


Figure 12: The relation of meteoroid bulk density, size, and mechanical strength represented by the dynamic pressure at 90% mass loss for three meteor showers and some sporadic fireballs with radiants in Virgo. Symbol size is proportional to meteoroid size. Different showers are distinguished by different colors.

been set reasonably well. The uncertainties of densities, assuming that other parameters are roughly correct, are about 10%.

The resulting densities in relation with the dynamic pressure at 90% mass loss and meteoroid size are shown in Fig. 12. For comparison, Taurids, κ -Cygnids, and some of the meteoroids initially considered to be η -Virginids but later rejected are included as well. The 90% mass loss was taken instead of maximal pressure in order to better represent the meteoroid as a whole. The difference was significant for some large Taurids containing small stronger inclusions. The size (diameter) was computed from the determined mass and density assuming spherical shape.

We can see that many κ -Cygnids had very low densities between $100 - 500 \text{ kg m}^{-3}$. Some stronger κ -Cygnids had larger densities but no more than 1000 kg m^{-3} . Taurids had densities $200 - 1500 \text{ kg m}^{-3}$, in one case even 2000 kg m^{-3} . The typical density of η -Virginids was about 1500 kg m^{-3} . None had less than 1000 kg m^{-3} and one reached 2500 kg m^{-3} . We also tried to fit light curves and decelerations of the video observed η -Virginids using the erosion model for small meteoroids of Borovička et al. (2007). The resulting densities were about 2000 kg m^{-3} or larger. The seven sporadic meteoroids had very wide range of densities and strength confirming that they were of various origin. Two of them were compatible in material properties with η -Virginids but very likely by chance. One of them had radiant in region B and the other in region C.

This analysis shows that κ -Cygnids represent a very weak material, undoubtedly of cometary origin. The parent body is not known but the orbit is of a short-period comet type. The Taurids originate from comet 2P/Encke and represent a stronger cometary material. The main difference with κ -Cygnids is that Taurids contain small inclusions of higher strength and density. The properties of η -Virginids are different. The stream does not contain low-density fragile bodies. On the other hand, the densities and strengths do not reach the values typical for ordinary chondrites and their precursor meteoroids. But they are compatible with carbonaceous chondrites containing some porosity. For example, the Winchcombe CM2 meteoroid had the strength 0.6 MPa (McMullan et al., 2024) and the recovered meteorites had the bulk density 2090 kg m^{-3} (King et al., 2022). The original meteoroid could have a larger porosity and lower density. Since carbonaceous chondrites originate from C-type asteroids such as Bennu (Lauretta et al., 2024) and Ryugu (Yokoyama et al., 2023), η -Virginids are probably of asteroidal origin. The orbits of fireballs are compatible with that since they have aphelia well inside the Jupiter orbit (Fig. 8) and below the limiting value of 4.9 AU of Borovička et al. (2022a), despite the Tisserand parameter being about 2.9. In many aspects, η -Virginids are physically similar to Geminids, though their strengths is somewhat lower (Fig. 11b) and densities are also lower than that determined by various authors for Geminids (Babadzhanov and Kokhirova, 2009; Borovička et al., 2010; Henych et al., 2026).

7. Possible parent bodies

To investigate whether the meteoroid stream is associated with a known asteroid, i.e. that the meteor shower has a potential parent body, we performed orbital-similarity analyses using the criteria proposed by Southworth and Hawkins (1963) and by Drummond (1981). We also applied the Nesvorný method (Nesvorný and Vokrouhlický, 2006) as a complementary approach, since it weights the orbital elements differently from the classical D-criteria and is therefore sensitive to additional aspects of orbital proximity. In this context, the Nesvorný method is used to rank candidate parent bodies according to how closely their orbits match the mean orbital elements of the η -Virginids (considering the observed dispersion among the meteors). We compared these mean elements with those of approximately 1.4 million small bodies listed in the Minor Planet Center's catalog¹.

For each similarity method, we selected the 100 objects with the lowest criterion values and downloaded their orbital elements from the JPL HORIZONS system², adopting 2021 February 21 as the reference epoch. With the orbital data of the potential parent bodies synchronized in time, we recomputed the similarity parameters.

Assuming that the parent body's orbit may lie within the range of the meteoroid stream's orbital elements, we evaluated the minimum value of each similarity criterion for each candidate within this range, rather than using only the mean orbital elements. Table 2 presents the computed criteria for the five best parent body candidates for each method. The 2003 FB5 figures as the best candidate using all three methods. This body was considered a possible source of η -Virginids by Jenniskens (2023). The similarity of this object with the meteoroid stream reaches orders of magnitude lower than the other candidates. 2015 FP33 and 2025 FA15 are also strong candidates, reaching high similarity in two of the three methods.

8. Orbital evolution

To get an insight into long-term evolution of orbits of η -Virginids, a backward orbital integration for 5,000 years was done using the high order integrator IAS15 in the REBOUND package (Rein and Spiegel, 2015). Thousand clones with orbital elements covering the observed range of orbits of η -Virginid fireballs and their uncertainties were produced. The results are shown in Fig. 13. The semimajor axis, eccentricity, and perihelion distance are stable. The inclination, on the other hand, shows large variations. It can change from 5° to $20-40^\circ$ within few hundreds of years. The variations

¹<https://minorplanetcenter.net/iau/MPCORB.html>

²<https://ssd.jpl.nasa.gov/horizons/>

Table 2

Similarity of the best five candidates to parent body by Southworth-Hawkins, Nesvorný, and Drummond methods.

asteroid designation	Southworth & Hawkins
2003 FB5	0.000179
2010 VF	0.026141
2015 FP33	0.027765
2011 EF17	0.027822
2025 BC10	0.031426
asteroid designation	Drummond
2003 FB5	0.000481
2025 FA15	0.010379
2011 EF17	0.017692
2006 UF17	0.018344
2017 TF5	0.018456
asteroid designation	Nesvorný
2003 FB5	2.057
2015 FP33	96.085
2025 FA15	378.775
2023 VO	445.913
2011 EF17	738.176

seems to be periodic but since the periods are different for different clones, the picture becomes smeared in more distant past. The longitudes of the nodes and arguments of perihelia then cluster around two preferred values separated by 180° . These variations may affect the visibility of the shower from Earth at different epochs.

It is not possible to draw any deterministic conclusions about the past or future evolution of η -Virginids from these calculations, since the orbits of the clones diverge drastically over time and we do not know which clones represent real meteoroids best. Such an orbital dynamical behavior is expected once the meteors come from a Kirkwood gap region. It is, nevertheless, evident that stream meteoroids can remain in the 3:1 mean motion resonance with Jupiter for a long time. We checked not only that the semimajor axis corresponds to the resonance but also the resonance angles. Out of 22 fireballs, 20 showed libration around the critical angle (e.g. Gallardo, 2018).

Figure 14 shows the evolution of semimajor axis and inclination of candidate parent asteroids 2003 FB5, 2015 FP33, and 2025 FA15. Except small oscillations, semimajor axes remain stable. Inclinations show large variations but in case of 2003 FB5 they are much slower than in η -Virginids. In this respect, 2015 FP33 and 2025 FA15 are more likely to be related to η -Virginids. All three asteroids are relatively small and were observed for only about a week. Their albedos or spectra are not known. Assuming carbonaceous composition and thus low albedo (0.05), the diameter of 2003 FB5 is about 120 meters, of 2015 FP33 about half of that and of 2025 FA15 about 40 m. Their connection with η -Virginids remains uncertain. Similarly to η -Virginids, their aphelia lie well below 4.9 AU but the Tisserand parameters are consistent with the Jupiter-family comet region.

9. Conclusions

We have examined the η -Virginid meteoroid stream using data from the European Fireball Network and a double-station video experiment. We have confirmed the four year periodicity in the activity of the meteor shower. The orbital period of four years was directly measured for the fireballs. Somewhat surprisingly, fainter meteors showed longer periods. However, the video observations during three nights showed that the shower is poor in faint meteors. The statistics of orbits of faint meteors are thus small at this moment. There is a relatively wide range of perihelion distances but only a narrow interval of inclinations. Orbital integrations showed that the semimajor axis remains stable for thousands of years, probably thanks to the 3:1 mean motion resonance with Jupiter. On the other hand, the inclination is expected to exhibit large periodic variations, which seems to be at odds with the small spread of inclinations of the observed fireballs. This aspect deserves further investigation.

Eta-Virginid meteoroid stream

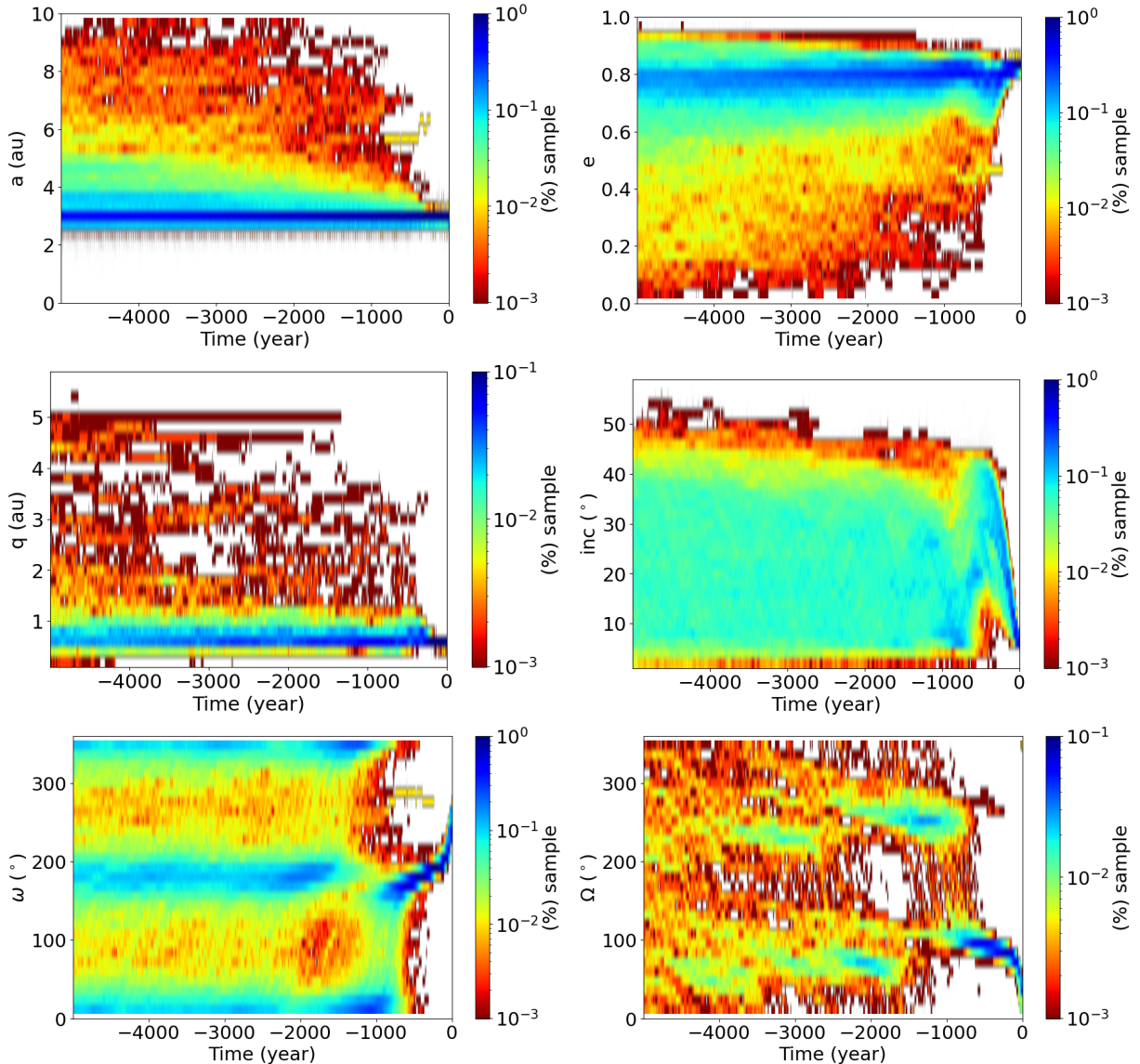


Figure 13: Results of backward orbital integration of η -Virginids for 5000 years. The fraction of clones is color coded. From upper left to lower right: semimajor axis, eccentricity, perihelion distance, inclination, argument of perihelion, longitude of the ascending node.

The physical properties of the meteoroids are different from cometary streams and are similar to the Geminids. The limiting fragmentation strength of 0.5 MPa and typical bulk density of cm-sized meteoroids of 1500 kg m^{-3} are somewhat lower than for Geminids but still suggest that the parent body is a carbonaceous asteroid. Some small meteoroids have densities around 2500 kg m^{-3} . Asteroids 2003 FB5, 2015 FP33, and 2025 FA15 were identified as those with most similar orbits to η -Virginids but a genetic relationship could not be proven. In any case, η -Virginids is another stream of asteroidal origin, in addition to the Geminids (and Daytime Sextantids related to them). Since η -Virginids do not approach the Sun so closely as Geminids, and their perihelion distance is stable, their high strength and density cannot be ascribed to solar proximity, strengthening the argument for asteroidal origin. The process of the stream formation remains, nevertheless, unknown.

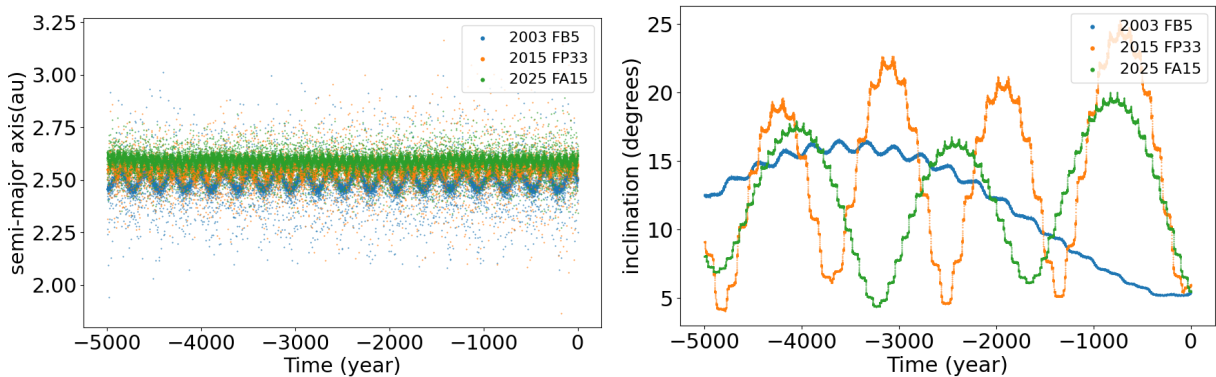


Figure 14: Evolution of semimajor axis and inclination of asteroids 2003 FB5, 2015 FP33, and 2025 FA15 from backward orbital integration.

CRediT authorship contribution statement

Jiří Borovička: Conceptualization, Methodology, Software, Formal analysis, Investigation, Writing - Original Draft, Visualization, Project administration, Funding acquisition. **Pavel Spurný:** Investigation, Formal analysis, Funding acquisition. **Pavel Koten:** Investigation, Formal analysis. **Gabriel Borderes Motta:** Formal analysis, Visualization. **Lenka Kotková:** Data Curation. **Rostislav Štork:** Resources. **Dušan Tomko:** Resources. **Thomas Weiland:** Resources.

Declaration of competing interest

The authors declare that they have no known competing financial interests or personal relationships that could have appeared to influence the work reported in this paper.

Acknowledgments

This work was supported by grant no. 24-10143S from the Czech Science Foundation. The operation of Slovak DAFOs was supported by Slovak Grant Agency for Science VEGA (grant no. 2/0067/26).

A. Appendix

The radiants and orbits of all individual η -Virginids are given in Table 3. The formal errors can be found in the Supplementary Material. The masses, densities, and fragmentation pressures derived from the fragmentation modeling are given in Table 4 for fireballs, which could be modeled. The zenith distance of the radiant, describing trajectory slope in the atmosphere, is also provided.

Data availability

More detailed data about the trajectories and orbits of fireballs used in this study (not only η -Virginids) are provided in the Supplementary Material to this article. For the modeled fireballs, the source data for modeling are also provided. They include the dynamic data (time-length-height), photographic, and radiometric light curves. The file Virgo-fireball-list.xlsx contains catalog data for 118 fireballs and 8 video meteors with radiants in the Virgo region in a similar manner as was provided for 824 fireballs in Borovička et al. (2022b). Fireball classification (PE and Pf numbers) cannot be used for video meteors and is not provided for them. Physical data such as photometric masses are given on the basis of global examination. Fragmentation modeling can later refine the values. Files EVI-dynamics.xlsx, EVI-photometry.xlsx, and EVI-radiometers.xlsx contain dynamic data, light curves, and radiometric light curves, respectively, for 13 fireballs from Table 4. Each fireball has a separate list where data from one or more cameras are given.

References

Babadzhanov, P.B., Kokhirova, G.I., 2009. Densities and porosities of meteoroids. *Astron. Astrophys.* 495, 353–358. doi:10.1051/0004-6361:200810460.

Borovička, J., Koten, P., Spurný, P., Čapek, D., Shrbený, L., Štork, R., 2010. Material properties of transition objects 3200 Phaethon and 2003 EH₁, in: Fernandez, J.A., Lazzaro, D., Prialnik, D., Schulz, R. (Eds.), *Icy Bodies of the Solar System*, pp. 218–222. doi:10.1017/S174392131000178X.

Borovička, J., Spurný, P., 2020. Physical properties of Taurid meteoroids of various sizes. *Planet. Space Sci.* 182, 104849. doi:10.1016/j.pss.2020.104849.

Borovička, J., Spurný, P., Koten, P., 2007. Atmospheric deceleration and light curves of Draconid meteors and implications for the structure of cometary dust. *Astron. Astrophys.* 473, 661–672. doi:10.1051/0004-6361:20078131.

Borovička, J., Spurný, P., Kotková, L., Molau, S., Tomko, D., Weiland, T., 2025. The structure of κ Cygnid and August Draconid meteoroid streams. *Astron. Astrophys.* 695, A83. doi:10.1051/0004-6361/202453552, arXiv:2502.02178.

Borovička, J., Spurný, P., Shrbený, L., 2020. Two Strengths of Ordinary Chondritic Meteoroids as Derived from Their Atmospheric Fragmentation Modeling. *Astron. J.* 160, 42. doi:10.3847/1538-3881/ab9608.

Borovička, J., Spurný, P., Shrbený, L., 2022a. Data on 824 fireballs observed by the digital cameras of the European Fireball Network in 2017–2018. II. Analysis of orbital and physical properties of centimeter-sized meteoroids. *Astron. Astrophys.* 667, A158. doi:10.1051/0004-6361/202244197.

Borovička, J., Spurný, P., Shrbený, L., Štork, R., Kotková, L., Fuchs, J., Keclíková, J., Zichová, H., Mánek, J., Váchová, P., Macourková, I., Svoreň, J., Mucke, H., 2022b. Data on 824 fireballs observed by the digital cameras of the European Fireball Network in 2017–2018. I. Description of the network, data reduction procedures, and the catalog. *Astron. Astrophys.* 667, A157. doi:10.1051/0004-6361/202244184.

Brček, A., Borovička, J., Spurný, P., 2021. Orbital and physical properties of eta-Virginids from the data of the European Fireball Network. *WGN, Journal of the International Meteor Organization* 49, 98–101.

Burns, J.A., Lamy, P.L., Soter, S., 1979. Radiation forces on small particles in the solar system. *Icarus* 40, 1–48. doi:10.1016/0019-1035(79)90050-2.

Cephecha, Z., McCrosky, R.E., 1976. Fireball end heights: A diagnostic for the structure of meteoric material. *J. Geophys. Res.* 81, 6257–6275. doi:10.1029/JB081i035p06257.

Cukier, W.Z., Szalay, J.R., 2023. Formation, Structure, and Detectability of the Geminids Meteoroid Stream. *Planet. Sci. J.* 4, 109. doi:10.3847/PSJ/acd538.

Drummond, J.D., 1981. A test of comet and meteor shower associations. *Icarus* 45, 545–553. URL: [http://dx.doi.org/10.1016/0019-1035\(81\)90020-8](http://dx.doi.org/10.1016/0019-1035(81)90020-8).

Gallardo, T., 2018. Resonances in the asteroid and trans-Neptunian belts: A brief review. *Planet. Space Sci.* 157, 96–103. doi:10.1016/j.pss.2018.03.007, arXiv:1803.06245.

Hajduková, M., Rudawska, R., Jopek, T.J., Koseki, M., Kokhirova, G., Neslušan, L., 2023. Modification of the Shower Database of the IAU Meteor Data Center. *Astron. Astrophys.* 671, A155. doi:10.1051/0004-6361/202244964.

Halliday, I., 1988. Geminid fireballs and the peculiar asteroid 3200 Phaethon. *Icarus* 76, 279–294. doi:10.1016/0019-1035(88)90073-5.

Henych, T., Borovička, J., Čapek, D., Vojáček, V., Spurný, P., Koten, P., Shrbený, L., 2026. Geminids are initially cracked by atmospheric thermal stress. *Astron. Astrophys.* in press.

Henych, T., Borovička, J., Vojáček, V., Spurný, P., 2024. Mechanical strength distribution in Geminid meteoroids derived via fireball modeling. *Astron. Astrophys.* 683, A229. doi:10.1051/0004-6361/202348797.

Jacchia, L.G., Whipple, F.L., 1961. Precision Orbits of 413 Photographic Meteors. *Smithsonian Contributions to Astrophysics* 4, 97–129.

Jenniskens, P., 2006. Meteor Showers and their Parent Comets. Cambridge University Press.

Jenniskens, P., 2023. *Atlas of Earth's Meteor Showers*. Elsevier.

Jenniskens, P., Nénon, Q., Albers, J., Gural, P.S., Haberman, B., Holman, D., Morales, R., Grigsby, B.J., Samuels, D., Johannink, C., 2016. The established meteor showers as observed by CAMS. *Icarus* 266, 331–354. doi:10.1016/j.icarus.2015.09.013.

Jewitt, D., Li, J., 2010. Activity in Geminid Parent (3200) Phaethon. *Astron. J.* 140, 1519–1527. doi:10.1088/0004-6256/140/5/1519.

Jewitt, D., Li, J., Agarwal, J., 2013. The Dust Tail of Asteroid (3200) Phaethon. *Astrophys. J. Lett.* 771, L36. doi:10.1088/2041-8205/771/2/L36.

Jo, H., Ishiguro, M., 2024. Dynamical study of Geminid formation assuming a rotational instability scenario. *Astron. Astrophys.* 683, A68. doi:10.1051/0004-6361/202347898.

King, A.J., Daly, L., Rowe, J., Joy, K.H., Greenwood, R.C., Devillepoix, H.A.R., Suttle, M.D., Chan, Q.H.S., Russell, S.S., Bates, H.C., Bryson, J.F.J., Clay, P.L., Vida, D., Lee, M.R., O'Brien, Á., Hallis, L.J., Stephen, N.R., Tartèse, R., Sansom, E.K., Towner, M.C., Cupak, M., Shober, P.M., Bland, P.A., Findlay, R., Franchi, I.A., Verchovsky, A.B., Abernethy, F.A.J., Grady, M.M., Floyd, C.J., Van Ginneken, M., Bridges, J., Hicks, L.J., Jones, R.H., Mitchell, J.T., Genge, M.J., Jenkins, L., Martin, P.E., Sephton, M.A., Watson, J.S., Salge, T., Shirley, K.A., Curtis, R.J., Warren, T.J., Bowles, N.E., Stuart, F.M., Di Nicola, L., Györe, D., Boyce, A.J., Shaw, K.M.M., Elliott, T., Steele, R.C.J., Povinec, P., Laubenstein, M., Sanderson, D., Cresswell, A., Jull, A.J.T., Sýkora, I., Sridhar, S., Harrison, R.J., Willcocks, F.M., Harrison, C.S., Hallatt, D., Wozniakiewicz, P.J., Burchell, M.J., Alesbrook, L.S., Dignam, A., Almeida, N.V., Smith, C.L., Clark, B., Humphreys-Williams, E.R., Schofield, P.F., Cornwell, L.T., Spathis, V., Morgan, G.H., Perkins, M.J., Kacerek, R., Campbell-Burns, P., Colas, F., Zanda, B., Vernazza, P., Bouley, S., Jeanne, S., Hankey, M., Collins, G.S., Young, J.S., Shaw, C., Horak, J., Jones, D., James, N., Bosley, S., Shuttleworth, A., Dickinson, P., McMullan, I., Robson, D., Smedley, A.R.D., Stanley, B., Bassom, R., McIntyre, M., Suttle, A.A., Fleet, R., Bastiaens, L., Ihász, M.B., McMullan, S., Boazman, S.J., Dickeson, Z.I., Grindrod, P.M., Pickersgill, A.E., Weir, C.J., Suttle, F.M., Farrelly, S., Spencer, I., Naqvi, S., Mayne, B., Skilton, D., Kirk, D., Mounsey, A., Mounsey, S.E., Mounsey, S., Godfrey, P., Bond, L., Bond, V., Wilcock, C., Wilcock, H., Wilcock, R., 2022. The Winchcombe meteorite, a unique and pristine witness from the outer solar system. *Science Advances* 8, eabq3925. doi:10.1126/sciadv.abq3925.

Knight, M.M., Kokotanekova, R., Samarasinha, N.H., 2024. Physical and Surface Properties of Comet Nuclei from Remote Observations, in: Meech, K.J., Combi, M.R., Bockelée-Morvan, D., Raymodn, S.N., Zolensky, M.E. (Eds.), *Comets III*. University of Arizona Press, pp. 361–404.

doi:10.2458/azu_uapress_9780816553631-ch012.

Koseki, M., 2019. Legendary meteor showers: Studies on Harvard photographic results. *WGN, Journal of the International Meteor Organization* 47, 139–150.

Koten, P., Shrbený, L., Spurný, P., Borovička, J., Štork, R., Henych, T., Vojáček, V., Mánek, J., 2023. τ Herculid meteor shower in the night of 30/31 May 2022 and the meteoroid properties. *Astron. Astrophys.* 675, A70. doi:10.1051/0004-6361/202346537.

Lauretta, D.S., Connolly, H.C., Aebersold, J.E., Alexander, C.M.O., Ballouz, R.L., Barnes, J.J., Bates, H.C., Bennett, C.A., Blanche, L., Blumenfeld, E.H., Clemett, S.J., Cody, G.D., DellaGiustina, D.N., Dworkin, J.P., Eckley, S.A., Fouustoukos, D.I., Franchi, I.A., Glavin, D.P., Greenwood, R.C., Haenecour, P., Hamilton, V.E., Hill, D.H., Hiroi, T., Ishimaru, K., Jourdan, F., Kaplan, H.H., Keller, L.P., King, A.J., Koefoed, P., Kontogiannis, M.K., Le, L., Macke, R.J., McCoy, T.J., Milliken, R.E., Najorka, J., Nguyen, A.N., Pajola, M., Polit, A.T., Righter, K., Roper, H.L., Russell, S.S., Ryan, A.J., Sandford, S.A., Schofield, P.F., Schultz, C.D., Seifert, L.B., Tachibana, S., Thomas-Keppta, K.L., Thompson, M.S., Tu, V., Tusberti, F., Wang, K., Zega, T.J., Wolner, C.W.V., 2024. Asteroid (101955) Bennu in the laboratory: Properties of the sample collected by OSIRIS-REx. *Meteorit. Planet. Sci.* 59, 2453–2486. doi:10.1111/maps.14227, arXiv:2404.12536.

Lindblad, B.A., 1971. A computerized stream search among 2401 photographic meteor orbits. *Smithsonian Contributions to Astrophysics* 12, 14–24.

McCrosky, R.E., Posen, A., 1961. Orbital Elements of Photographic Meteors. *Smithsonian Contributions to Astrophysics* 4, 15–84.

McMullan, S., Vida, D., Devillepoix, H.A.R., Rowe, J., Daly, L., King, A.J., Cupák, M., Howie, R.M., Sansom, E.K., Shober, P., Towner, M.C., Anderson, S., McFadden, L., Horák, J., Smedley, A.R.D., Joy, K.H., Shuttleworth, A., Colas, F., Zanda, B., O'Brien, Á.C., McMullan, I., Shaw, C., Suttle, A., Suttle, M.D., Young, J.S., Campbell-Burns, P., Kacerek, R., Bassom, R., Bosley, S., Fleet, R., Jones, D., McIntyre, M., James, N., Robson, D., Dickinson, P., Bland, P.A., Collins, G.S., 2024. The Winchcombe fireball—That lucky survivor. *Meteorit. Planet. Sci.* 59, 927–947. doi:10.1111/maps.13977, arXiv:2303.12126.

Nesvorný, D., Vokrouhlický, D., 2006. New candidates for recent asteroid breakups. *The Astronomical Journal* 132, 1950–1958. URL: <http://dx.doi.org/10.1086/507989>, doi:10.1086/507989.

Rein, H., Spiegel, D.S., 2015. IAS15: a fast, adaptive, high-order integrator for gravitational dynamics, accurate to machine precision over a billion orbits. *Mon. Not. R. Astron. Soc.* 446, 1424–1437. doi:10.1093/mnras/stu2164, arXiv:1409.4779.

Rybářová, G.O., 2016. A preliminary numerical model of the Geminid meteoroid stream. *Mon. Not. R. Astron. Soc.* 456, 78–84. doi:10.1093/mnras/stv2626.

Shiba, Y., 2018. Eta Virginids (EVI) four year cycle. *WGN, Journal of the International Meteor Organization* 46, 184–190.

Shiba, Y., 2022. Jupiter Family Meteor Showers by SonotaCo Network Observations. *WGN, Journal of the International Meteor Organization* 50, 38–61.

Southworth, R.B., Hawkins, G.S., 1963. Statistics of meteor streams. *Smithsonian Contributions to Astrophysics* 7, 261–285.

Spurný, P., 1993. Geminids from photographic records, in: Štohl, J., Williams, I.P. (Eds.), *Meteoroids and their Parent Bodies*, Astron. Inst. Slovak Acad. Sci.. pp. 193–196.

Spurný, P., Borovička, J., Mucke, H., Svoreň, J., 2017. Discovery of a new branch of the Taurid meteoroid stream as a real source of potentially hazardous bodies. *Astron. Astrophys.* 605, A68. doi:10.1051/0004-6361/201730787.

Trigo-Rodríguez, J.M., Llorca, J., 2006. The strength of cometary meteoroids: clues to the structure and evolution of comets. *Mon. Not. R. Astron. Soc.* 372, 655–660. doi:10.1111/j.1365-2966.2006.10843.x.

Whipple, F.L., 1954. Photographic meteor orbits and their distribution in space. *Astron. J.* 59, 201. doi:10.1086/106998.

Ye, Q., Jenniskens, P., 2024. Comets and Meteor Showers, in: Meech, K.J., Combi, M.R., Bockelée-Morvan, D., Raymodn, S.N., Zolensky, M.E. (Eds.), *Comets III*. University of Arizona Press, pp. 799–822. doi:10.2458/azu_uapress_9780816553631-ch024.

Yokoyama, T., Nagashima, K., Nakai, I., Young, E.D., Abe, Y., Aléon, J., Alexander, C.M.O., Amari, S., Amelin, Y., Bajo, K.i., Bizzarro, M., Bouvier, A., Carlson, R.W., Chaussidon, M., Choi, B.G., Dauphas, N., Davis, A.M., Di Rocca, T., Fujiya, W., Fukai, R., Gautam, I., Haba, M.K., Hibiya, Y., Hidaka, H., Homma, H., Hoppe, P., Huss, G.R., Ichida, K., Iizuka, T., Ireland, T.R., Ishikawa, A., Ito, M., Itoh, S., Kawasaki, N., Kita, N.T., Kitajima, K., Kleine, T., Komatani, S., Krot, A.N., Liu, M.C., Masuda, Y., McKeegan, K.D., Morita, M., Motomura, K., Moynier, F., Nguyen, A., Nittler, L., Onose, M., Pack, A., Park, C., Piani, L., Qin, L., Russell, S.S., Sakamoto, N., Schönbächler, M., Tafta, L., Tang, H., Terada, K., Terada, Y., Usui, T., Wada, S., Wadhwa, M., Walker, R.J., Yamashita, K., Yin, Q.Z., Yoneda, S., Yui, H., Zhang, A.C., Connolly, H.C., Lauretta, D.S., Nakamura, T., Naraoka, H., Noguchi, T., Okazaki, R., Sakamoto, K., Yabuta, H., Abe, M., Arakawa, M., Fujii, A., Hayakawa, M., Hirata, N., Hirata, N., Honda, R., Honda, C., Hosoda, S., Iijima, Y.i., Ikeda, H., Ishiguro, M., Ishihara, Y., Iwata, T., Kawahara, K., Kikuchi, S., Kitazato, K., Matsumoto, K., Matsuoka, M., Michikami, T., Mimasu, Y., Miura, A., Morota, T., Nakazawa, S., Namiki, N., Noda, H., Noguchi, R., Ogawa, N., Ogawa, K., Okada, T., Okamoto, C., Ono, G., Ozaki, M., Saiki, T., Sakatani, N., Sawada, H., Senshu, H., Shimaki, Y., Shirai, K., Sugita, S., Takei, Y., Takeuchi, H., Tanaka, S., Tatsumi, E., Terui, F., Tsuda, Y., Tsukizaki, R., Wada, K., Watanabe, S.i., Yamada, M., Yamada, T., Yamamoto, Y., Yano, H., Yokota, Y., Yoshihara, K., Yoshikawa, M., Yoshikawa, K., Furuya, S., Hatakeyama, K., Hayashi, T., Hitomi, Y., Kumagai, K., Miyazaki, A., Nakato, A., Nishimura, M., Soejima, H., Suzuki, A., Yada, T., Yamamoto, D., Yogata, K., Yoshitake, M., Tachibana, S., Yurimoto, H., 2023. Samples returned from the asteroid Ryugu are similar to Ivuna-type carbonaceous meteorites. *Science* 379, abn7850. doi:10.1126/science.abn7850.

Zhang, Q., Battams, K., Ye, Q., Knight, M.M., Schmidt, C.A., 2023. Sodium Brightening of (3200) Phaethon near Perihelion. *Planet. Sci. J.* 4, 70. doi:10.3847/PSJ/acc366.

Table 3

Radiants and orbits of individual η -Virginids (J2000.0). The given quantities are fireball or meteor code, solar longitude, geocentric radiant and velocity, semimajor axis, eccentricity, perihelion distance, inclination, argument of perihelion, and longitude of ascending node.

Code	λ_{\odot}	α_g	δ_g	v_g	a	e	q	i	ω	Ω
EN140317_194345	354.1817	181.66	5.31	26.51	2.507	0.812	0.470	5.30	280.13	354.181
EN150317_0158	354.4408	182.39	5.29	26.60	2.46	0.811	0.464	5.62	280.96	354.441
EN150317_233402	355.3370	186.58	2.25	29.40	2.53	0.851	0.378	5.49	290.40	355.337
EN120318_231735	352.0788	179.72	6.37	26.54	2.546	0.815	0.472	5.48	279.75	352.078
EN100321_191736	350.1501	178.19	5.61	26.88	2.498	0.818	0.456	4.36	281.72	350.147
EN140321_205321	354.2089	179.96	6.47	25.41	2.548	0.800	0.509	5.24	275.58	354.209
EN150321_011020	354.3868	182.19	4.69	26.68	2.471	0.813	0.462	5.03	281.23	354.387
EN150321_232628	355.3116	186.00	2.76	28.79	2.49	0.842	0.395	5.55	288.64	355.312
EN210321_003342	360.3323	188.77	2.31	27.65	2.583	0.830	0.438	5.78	283.59	0.335
EN230321_013723	362.3614	190.24	1.45	27.35	2.541	0.823	0.445	5.47	282.99	2.365
EN180322_232513	358.0373	185.64	3.78	26.85	2.538	0.818	0.462	5.59	281.06	358.039
EN190322_034625	358.2177	188.70	1.91	28.74	2.480	0.840	0.396	5.85	288.56	358.219
EN210322_191719	360.8468	187.74	2.50	26.64	2.54	0.815	0.468	5.19	280.37	0.850
EN210322_232919	361.0206	188.79	2.06	27.32	2.574	0.826	0.448	5.43	282.47	1.024
EN170325_224228	357.2379	186.84	3.06	28.04	2.495	0.832	0.420	5.90	285.83	357.239
EN190325_013833	358.3538	187.33	2.73	27.78	2.517	0.829	0.430	5.67	284.69	358.356
EN190325_024116	358.3971	183.56	4.57	25.41	2.557	0.801	0.510	4.97	275.56	358.399
EN200325_014301	359.3508	187.69	2.91	27.34	2.517	0.823	0.445	5.81	283.03	359.353
EN200325_024052	359.3907	188.81	2.04	28.26	2.554	0.837	0.419	5.79	286.03	359.393
EN200325_182414	360.0415	187.40	2.85	26.81	2.525	0.817	0.462	5.43	281.07	0.045
EN210325_042444	360.4557	188.14	2.07	27.04	2.484	0.818	0.451	5.08	282.44	0.459
EN210325_225915	361.2241	188.52	2.40	26.79	2.517	0.816	0.462	5.46	281.12	1.228
25318040	358.2515	186.72	3.16	28.35	2.89	0.850	0.433	5.89	283.30	358.253
25318057	358.3482	187.85	2.47	28.81	2.77	0.851	0.412	5.94	286.01	358.350
25320049	360.3097	188.72	2.11	27.64	2.55	0.829	0.437	5.58	283.79	0.313
25320055	360.3180	188.67	2.13	27.99	2.70	0.839	0.434	5.65	283.66	0.321

Table 4

Physical parameters of modeled η -Virginid fireballs. The given quantities are fireball code, initial mass, density, zenith distance of the radiant, dynamic pressure at the first fragmentation, at the time of 90% mass loss, and the maximum reached pressure. Mass is in grams, density in kg m^{-3} , and pressures in kPa.

Code	m	ρ	z_R	p_1	$p_{90\%}$	p_{\max}
EN140317_194345	4.5	1200	62°	3.3	76	97
EN120318_231735	2.8	1800	41	1.7	140	190
EN100321_191736	5.0	1750	68	1.2	110	120
EN140321_205321	1.7	1600	51	1.4	88	100
EN150321_011020	5.1	1700	48	3.8	130	180
EN210321_003342	73	1800	45	96	580	610
EN230321_013723	17.5	1450	52	1.8	300	310
EN190322_034625	53	2500	67	5.2	470	510
EN170325_224228	2.3	1650	47	0.8	190	190
EN190325_013833	13	1100	52	1.5	29	130
EN200325_014301	260	1300	49	60	370	440
EN210325_042444	3200	1500	75	13	350	490
EN210325_225915	2.2	1400	45	1.7	200	200